View metadata, citation and similar papers at core.ac.uk
brought to you by CORE
provided by Elsevier - Publisher Connector

Cell PRESS
Cell Host & Microbe
Article

Receptor-like Cytoplasmic Kinases Integrate Signaling from Multiple Plant Immune Receptors and Are Targeted by a *Pseudomonas syringae* Effector

Jie Zhang,[1,4] Wei Li,[1,4] Tingting Xiang,[1,2] Zixu Liu,[1] Kristin Laluk,[3] Xiaojun Ding,[1] Yan Zou,[1] Minghui Gao,[1] Xiaojuan Zhang,[1] She Chen,[1] Tesfaye Mengiste,[3] Yuelin Zhang,[1] and Jian-Min Zhou[1,*]
[1]National Institute of Biological Sciences, Beijing 102206, China
[2]State Key Laboratory of Plant Physiology and Biochemistry, College of Biological Sciences, China Agricultural University, Beijing 100094, China
[3]Department of Botany and Plant Pathology, Purdue University, West Lafayette, IN 47907, USA
[4]These authors contributed equally to this work
*Correspondence: zhoujianmin@nibs.ac.cn
DOI 10.1016/j.chom.2010.03.007

SUMMARY

Cell-surface-localized plant immune receptors, such as FLS2, detect pathogen-associated molecular patterns (PAMPs) and initiate PAMP-triggered immunity (PTI) through poorly understood signal-transduction pathways. The pathogenic *Pseudomonas syringae* effector AvrPphB, a cysteine protease, cleaves the *Arabidopsis* receptor-like cytoplasmic kinase PBS1 to trigger cytoplasmic immune receptor RPS5-specified effector-triggered immunity (ETI). Analyzing the function of AvrPphB in plants lacking *RPS5*, we find that AvrPphB can inhibit PTI by cleaving additional PBS1-like (PBL) kinases, including BIK1, PBL1, and PBL2. In unstimulated plants, BIK1 and PBL1 interact with FLS2 and are rapidly phosphorylated upon FLS2 activation by its ligand flg22. Genetic and molecular analyses indicate that BIK1, and possibly PBL1, PBL2, and PBS1, integrate immune signaling from multiple immune receptors. Whereas AvrPphB-mediated degradation of one of these kinases, PBS1, is monitored by RPS5 to initiate ETI, this pathogenic effector targets other PBL kinases for PTI inhibition.

INTRODUCTION

Plants use a suite of cell-surface-localized pattern-recognition receptors to detect various pathogen/microbe-associated molecular patterns (PAMPs/MAMPs) and trigger immune responses (Schwessinger and Zipfel, 2008). PAMP-triggered immunity (PTI) is critical for the survival of land plants under constant threat from numerous potential pathogenic microbes. The signal-transduction mechanism underlying PTI, however, is not well understood. The best-studied PTI pathway is initiated by the receptor kinase FLS2. Upon binding to the bacterial flagellar peptide flg22 (Chinchilla et al., 2006), FLS2 rapidly associates with another receptor-like kinase, BAK1, to activate defenses (Chinchilla et al., 2007; Heese et al., 2007). Similarly, the receptor kinase EFR binds the bacterial elongation factor-Tu (EF-Tu) peptide elf18 to trigger immune responses (Zipfel et al., 2006). Another receptor-like kinase, CERK1, is required for defenses in response to chitin, a fungal cell-wall component. CERK1 possesses three LysM domains that are thought to bind chitin (Miya et al., 2007; Wan et al., 2008). CERK1 is also required for plant resistance to the bacterial pathogen *Pseudomonas syringae* (Gimenez-Ibanez et al., 2009), although the corresponding PAMP remains to be identified. Downstream, two MAP kinase cascades are activated. MEKK1, MKK1, MKK2, and MPK4 constitute a cascade negatively regulating PTI defenses (Ichimura et al., 2006; Qiu et al., 2008; Suarez-Rodriguez et al., 2007), whereas MPK3 and MPK6 are thought to positively regulate PTI defenses (Schwessinger and Zipfel, 2008). We have no knowledge of additional components that act in early phases of the signal transduction. Furthermore, it is not known how signals from distinct immune receptors are integrated to activate an overlapping set of downstream defense responses.

P. syringae secretes a large number of effector proteins into host cells to assist its proliferation in plants (Cunnac et al., 2009). Many of these effector proteins are capable of targeting components of the PTI signaling pathway to suppress plant immunity (Block et al., 2008; Fu et al., 2007; Gimenez-Ibanez et al., 2009; Göhre et al., 2008; Kim et al., 2005; Li et al., 2005; Nomura et al., 2006; Xiang et al., 2008; Zhang et al., 2007; Zhou and Chai, 2008). For example, the *P. syringae* effector AvrPto acts as a kinase inhibitor to directly block immune signaling from FLS2 and EFR (Xiang et al., 2008). Another *P. syringae* effector, AvrPtoB, structurally and functionally mimics E3 ubiquitin ligase (Janjusevic et al., 2006; Abramovitch et al., 2006) and inhibits PTI by targeting FLS2 (Göhre et al., 2008) and CERK1 (Gimenez-Ibanez et al., 2009) for degradation. Shan et al. (2008) suggested that both AvrPto and AvrPtoB target BAK1. In addition, the *P. syringae* effector HopAI1 uses phosphothreonine lyase activity to "dephosphorylate" *Arabidopsis* MPK3 and MPK6, thereby permanently inactivating the MAP kinases (Zhang et al., 2007). The fact that many of the *P. syringae* effectors target important signaling components to inhibit PTI suggests that they can be used as powerful molecular probes

to identify PTI signaling components. Indeed, analyses of host targets for the *P. syringae* effectors HopU1 and HopM1 have led to the identification of GRP7 and MIN7 as mediators of plant immunity (Fu et al., 2007; Nomura et al., 2006).

Some pathogen effectors trigger immunity mediated by cytoplasmic immune receptors that are primarily nucleotide-binding, leucine-rich repeat (NB-LRR) proteins. The recognition of effectors by NB-LRR proteins is often indirectly mediated by other host proteins of diverse biochemical functions (Jones and Dangl, 2006). For example, the recognition of AvrPto by the NB-LRR protein Prf in tomato plants is mediated by the protein kinase Pto (Mucyn et al., 2006; Tang et al., 1996). Likewise, the *P. syringae* effector AvrPphB, a cysteine protease, triggers RPS5-specified disease resistance by proteolytically cleaving the cytoplasmic receptor-like kinase PBS1 (Ade et al., 2007; Shao et al., 2003). Thus, the Prf-Pto and RPS5-PBS1 protein complexes act as a conformational switch that is activated only when the corresponding effector proteins are present. However, it is not understood why different host proteins are deployed as sensors for effector-triggered immunity (ETI).

Here we show that AvrPphB inhibits PTI when directly expressed in plants. Interestingly, AvrPphB is capable of proteolytically cleaving a number of PBS1-like (PBL) proteins belonging to the subfamily VII of cytoplasmic receptor-like protein kinases. One of the PBL proteins, BIK1, is required for signaling elicited by flg22, elf18, and chitin and is essential for PAMP-induced resistance to *P. syringae*. Other members including PBL1, PBL2, and PBS1 also contribute to PTI defenses. BIK1 interacts with FLS2, EFR, and CERK1 in unstimulated plants. Treatment of plants with flg22 induces BIK1 phosphorylation in an FLS2- and BAK1-dependent manner. These results indicate that these kinases, particularly BIK1, play a central role in signal integration from multiple surface-localized receptors.

RESULTS

Transgenic AvrPphB Inhibits PTI Signaling

We used a protoplast-based reporter assay (Li et al., 2005; Xiang et al., 2008) to determine whether flg22-induced expression of *FRK1*, a PTI marker gene, can be inhibited by the expression of the *AvrPphB* transgene. Flg22 induces the expression of *FRK1* promoter-firefly luciferase reporter gene (*FRK1::LUC*; Figure 1A). The presence of AvrPphB reduced *FRK1::LUC* expression by 80%, but the protease-compromised AvrPphB^{C98S} mutant (cysteine 98 to serine; Shao et al., 2003) was largely unable to inhibit *FRK1::LUC* expression (Figure 1A; see Figure S1A available online). To further determine whether AvrPphB possesses PTI-inhibitory activity, we introduced a FLAG-tagged *AvrPphB* transgene into the *Arabidopsis rps5-2* mutant. *Arabidopsis* plants exposed to various PAMPs deposit callose at the cell wall and develop a rapid oxidative burst exemplified by the accumulation of H_2O_2 (Felix et al., 1999; Gómez-Gómez et al., 1999; Kunze et al., 2004; Miya et al., 2007). The flg22-induced H_2O_2 accumulation in T1 *AvrPphB* transgenic plants was reduced to 25% compared with the nontransgenic *rps5* control (Figure 1B). Two independent transgenic lines in the T3 generation were further tested for oxidative burst and callose deposition in response to flg22, elf18, and chitin. H_2O_2 accumulation in the two *AvrPphB* transgenic lines was consistently reduced to 20%–40% compared with nontransgenic *rps5* control (Figures 1C–1E). Similarly, PAMP-induced callose deposition in *AvrPphB* transgenic plants was also reduced to 40%–50% compared with control plants (Figure 1F). Together, these results indicated that AvrPphB is capable of inhibiting signaling from all three PAMPs.

PBS1-like Kinases Are AvrPphB Substrates

The cleavage of PBS1 does not appear to account for the PTI-inhibition activity of AvrPphB, because our initial analysis of *pbs1* mutants showed only minimal defects in PTI defenses. As expected, an immunoblot experiment did not detect a cleavage or reduction in abundance of FLS2 in *AvrPphB* transgenic plants (Figure S1B). We therefore hypothesized that AvrPphB may target additional host proteins homologous to PBS1 for PTI inhibition. PBS1 belongs to receptor-like cytoplasmic kinase (RLCK) subfamily VII. The amino acid sequences of the 45 RLCK VII members were therefore aligned and analyzed for the AvrPphB recognition sequence (Figure S2A). In total, we identified 29 putative PBL proteins as potential substrates for AvrPphB. One of the PBL proteins is BIK1, an RLCK required for resistance to *Botrytis cinerea* (Veronese et al., 2006). The remaining PBL proteins are named PBL1–PBL28. The putative AvrPphB substrates were fused to an HA tag and transiently expressed in *Arabidopsis rps5* mutant protoplasts along with AvrPphB. The coexpression of AvrPphB resulted in cleavage of nine of the ten selected proteins (Figure 2A). PBL6, which contains a D-to-S substitution in the GDK motif, was not cleaved. PBL1, which contains a D-to-E substitution in the GDK motif, was cleaved normally, suggesting that an acidic residue in the GDK motif is required for the cleavage. These results are consistent with a previous report that a D-to-A substitution in the GDK motif of PBS1 reduces AvrPphB cleavage by 75% (Shao et al., 2003). BSK1, an RLCK XII family member involved in brassinosteroid signaling (Tang et al., 2008), was not cleaved by AvrPphB, indicating that AvrPphB specifically targets PBS1 and PBL proteins. The protease-compromised AvrPphB mutant did not cleave BIK1 (Figure S2B). To determine whether the AvrPphB protein delivered from the *P. syringae* bacteria is capable of cleaving BIK1, we generated transgenic lines expressing HA-tagged BIK1 under the control of the *BIK1* native promoter in the *rps5* mutant background. Inoculation of *BIK1::BIK1-HA* plants with *P. syringae* carrying *avrPphB* produced a cleaved product, whereas the plants inoculated with the *P. syringae* strain lacking *avrPphB* did not (Figure 2B).

An examination of public microarray data indicated that *BIK1*, *PBL1*, and *PBL2* transcripts are strongly upregulated by flg22. Quantitative RT-PCR confirmed this result with flg22 treatment inducing *BIK1*, *PBL1*, and *PBL2* transcripts by 2.5- to 5.5-fold compared with an H_2O-treated control (Figure S3A). A small but statistically significant induction of *PBS1* by flg22 was also observed. These results suggest that the PBL genes are linked to PTI defenses.

Flg22 Induces BIK1 Phosphorylation

An examination of the protoplast-expressed BIK1 and the PBL1 proteins showed a slower migration following flg22 treatment (Figure 3A). Treatment of the protein samples with a protein

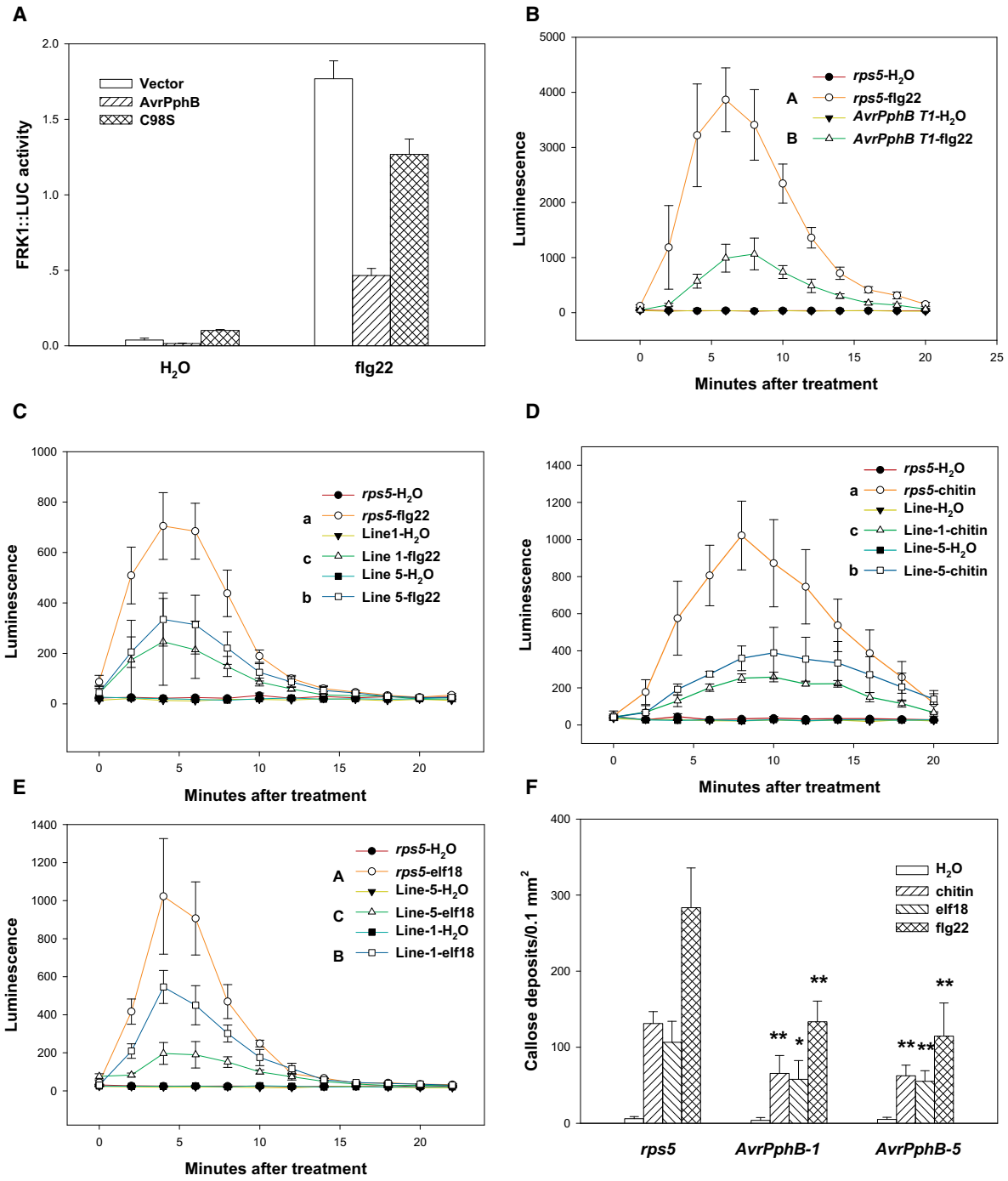

Figure 1. Transgenic Expression of AvrPphB Inhibits PAMP-Induced Defenses

(A) Transient expression of AvrPphB inhibits flg22-induced *FRK1::LUC* expression. *rps5* protoplasts were transfected with *FRK1::LUC* along with WT AvrPphB-FLAG, AvrPphB^{C98S}-FLAG mutant construct, or an empty vector, induced with flg22, and the *LUC* reporter activity was determined. Values were normalized to an internal *35S::RLUC* control.

(B–F) Stable transgenic *AvrPphB* inhibits PAMP-induced defenses. Flg22-induced H_2O_2 production was reduced in T1 transgenic plants (B). Flg22-, elf18-, and chitin-induced H_2O_2 production (C–E) and callose deposition (F) were diminished in *AvrPphB* transgenic lines 1 and 5. The results shown are representative of three independent experiments. Each data point consists of four replicates. Error bars indicate standard deviation. Student's *t* test was carried out to determine the significance of the difference between the *AvrPphB* transgenic plants and nontransgenic control in the same treatment. * or lowercase letters indicate a significant difference at $p < 0.05$, whereas ** or capital letters indicate a significant difference at $p < 0.01$.

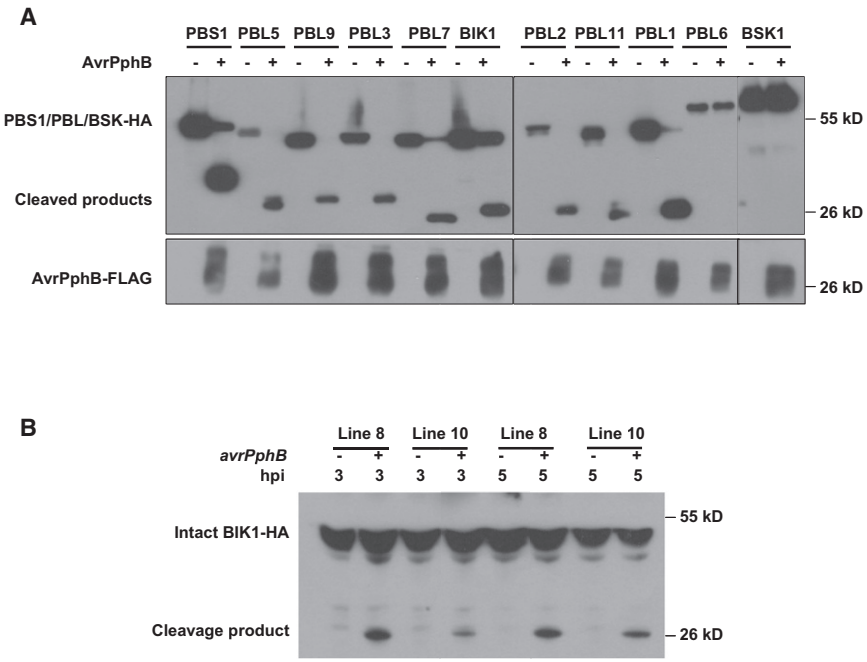

Figure 2. PBS1-like Kinases Are Substrates for the AvrPphB Protease

(A) PBL proteins are proteolytically cleaved by AvrPphB in protoplasts. HA-tagged PBS1, BIK1, PBLs, and BSK1 were coexpressed with AvrPphB-FLAG in *rps5* protoplasts. Intact and cleaved products of the kinases were detected by anti-HA immunoblot, and the AvrPphB-FLAG protein was detected by anti-FLAG immunoblot.

(B) Bacterially delivered AvrPphB cleaves BIK1 in plants. *BIK1::BIK1-HA* transgenic lines (in the *rps5* background) were infiltrated with 10^8 cfu/ml *P. syringae* DC3000 bacteria with (+) or without (–) *avrPphB*, and the presence of cleaved BIK1-HA product was determined at the indicated hours postinoculation (hpi).

phosphatase completely restored normal migration to both BIK1 and PBL1, indicating that these proteins were phosphorylated after flg22 treatment. The phosphorylation is transient in nature because BIK1 migrated normally 20 min after flg22 treatment (Figure 3B). Flg22 failed to induce BIK1 phosphorylation in *fls2* protoplasts (Figure 3B). Transfection of *fls2* protoplasts with an FLS2-FLAG plasmid restored the flg22-induced BIK1 phosphorylation. Likewise, BIK1 was not phosphorylated in *bak1* mutant protoplasts (Figure 3C), indicating that both FLS2 and BAK1 are required for the flg22-induced phosphorylation of BIK1. The flg22-induced, *FLS2*-dependent phosphorylation was also observed in stable *BIK1::BIK1-HA* transgenic plants (Figure 3D). Together, the results indicate that the activation of FLS2 by flg22 induces a transient phosphorylation of BIK1 and PBL1.

We previously showed that AvrPto inhibits kinase activity of FLS2. Coexpression of WT AvrPto, but not AvrPto^{Y89D} mutant, which does not interact with FLS2, prevented the flg22-induced phosphorylation of BIK1 (Figure S3B), suggesting that the kinase activity of FLS2 is required for BIK1 phosphorylation in the protoplasts.

BIK1 Interacts with FLS2 and Dissociates from FLS2 following Flg22 Treatment

Because BIK1 is localized to the plasma membrane (Veronese et al., 2006) and phosphorylated rapidly in response to flg22, we asked whether BIK1 interacts with FLS2. A GST pull-down experiment showed that GST-BIK1, but not GST, interacted with the His-tagged FLS2 kinase domain in vitro (Figure 4A). Coimmunoprecipitation (co-IP) experiments in *BIK1::BIK1-HA* transgenic plants showed that BIK1 interacted with the endogenous FLS2 in plants (Figure 4B). We also coexpressed BIK1-HA with FLAG-tagged FLS2, EFR, BAK1, and CERK1 in *Arabidopsis* protoplasts and performed co-IP assays (Figure S4). A strong interaction of BIK1 with FLS2, EFR, and CERK1, but not BAK1, was observed. We detected a weak signal of BAK1-BIK1 association only in the presence of FLS2 and EFR overexpression in the same protoplasts (arrowhead; Figures S4A and S4C). These results indicate that BIK1 directly interacts with FLS2, and likely EFR and CERK1, in plants. Similarly, co-IP experiments in *PBL1::PBL1-HA* transgenic plants detected a PBL1-FLS2 interaction in plants (Figure 4B).

We further used the protoplast transient expression system to determine the effect of flg22 treatment on BIK1-FLS2 interaction. Surprisingly, flg22 treatment significantly reduced BIK1-FLS2 interaction (Figure 4C). We similarly detected a strong interaction of FLS2 with PBS1, PBL1, and PBL2 in the absence of flg22 treatment. In each case, the addition of flg22 also significantly reduced the interaction of FLS2 with PBS1 and the PBL proteins. These results suggest that BIK1, PBS1, and the two PBL proteins are associated with FLS2 in unstimulated cells, and that the activation of FLS2 by flg22 induces the dissociation of the protein complex. The flg22-induced BIK1 phosphorylation is less pronounced in these experiments, likely because of the presence of unknown phosphatases during the co-IP experiments. The unstable BIK1 phosphorylation is also consistent with the transient nature of BIK1 phosphorylation.

The flg22-induced BIK1 phosphorylation and BIK1-FLS2 dissociation prompted us to determine whether these two events are linked. Because BAK1 is required for the phosphorylation of BIK1, we examined the flg22-induced BIK1-FLS2 dissociation in *bak1* mutant protoplasts. Figure 4D shows that flg22 does not induce such dissociation in the *bak1* mutant, indicating that BAK1 is required for the dissociation. We further examined the dissociation in the presence of AvrPto. Coexpression of AvrPto, but not AvrPto^{Y89D}, prevented BIK1-FLS2 dissociation (Figure 4E). These results suggest that the flg22-induced phosphorylation of BIK1 is required for BIK1-FLS2 dissociation.

BIK1 and PBL1 Are Required for PAMP-Induced Defenses

The results described above suggest that BIK1, PBS1, and PBL proteins act downstream of FLS2, EFR, and CERK1 to mediate PTI signaling. To determine the function of BIK1 and PBS1 in PTI defenses, we first examined PAMP-induced H_2O_2

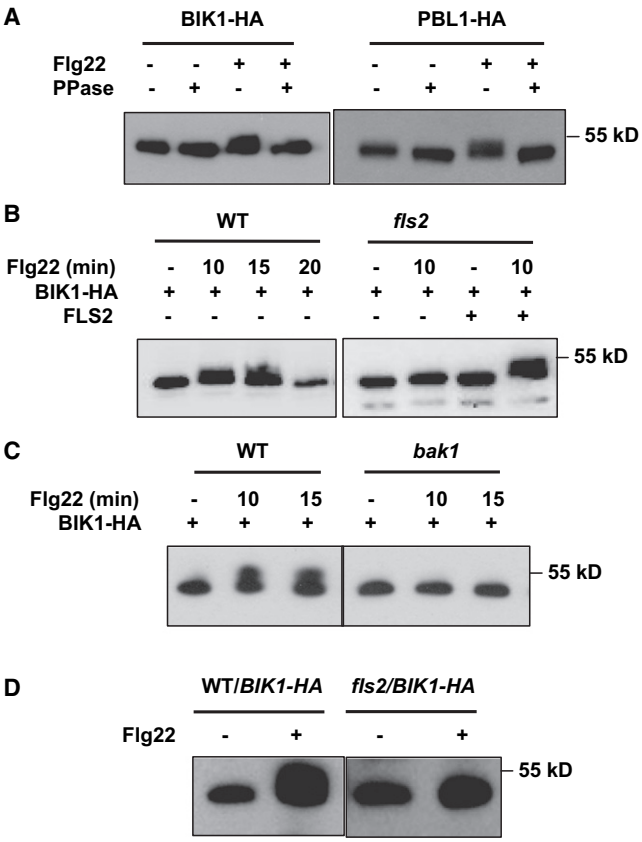

Figure 3. Flg22 Induces BIK1 and PBL1 Phosphorylation

(A) Flg22 induces a mobility shift of the BIK1 and PBL1 proteins.

(B) Flg22-induced BIK1 phosphorylation requires *FLS2*.

(C) Flg22-induced BIK1 phosphorylation requires *BAK1*. WT protoplasts (A) or protoplasts of the indicated genotypes (B) and (C) were transfected with the indicated constructs, treated with flg22 for the indicated times, and the migration of BIK1-HA or PBL1-HA proteins was examined by anti-HA immunoblot. Where indicated, protein was treated with λ protein phosphatase (PPase) prior to immunoblot analysis. For complementation, *fls2* protoplasts were cotransfected with an FLS2-FLAG construct (B).

(D) Flg22 induces BIK1 phosphorylation in plants. *BIK1::BIK1-HA* transgenic plants of the indicated genetic background were treated with flg22 for 10 min, and BIK1 migration was determined with anti-HA immunoblot. The results shown are representative of three independent experiments.

production in loss-of-function *bik1* (Veronese et al., 2006) and *pbs1-2* mutants (Warren et al., 1999). When treated with flg22, *bik1* consistently accumulated 50%–80% less H_2O_2 compared with WT, whereas the *fls2* mutant was completely unable to respond to flg22 (Figure 5A; Figure S5A). Similarly, elf18- and chitin-induced H_2O_2 production was also reduced to 20%–40% compared with WT (Figures 5B and 5C). The *pbs1* mutant frequently showed a minimal, but statistically significant, reduction in H_2O_2 accumulation (Figures 5A–5C). We next determined whether the *bik1* mutation affected PAMP-induced callose deposition at the cell wall. The *bik1* mutant showed only approximately 25%–50% callose deposits compared with WT, whereas the *fls2*, *efr*, and *cerk1* mutants had 10% or less callose deposits in response to the corresponding PAMPs (Figure 5D; Figures S5B–S5D). The *pbs1* mutant again displayed a small but statistically significant reduction of callose deposition (Figure 5D). Immunoblot analysis showed that FLS2 protein level was not affected by *bik1* and *pbs1* mutations (Figure S5E), indicating that the observed defects in PAMP signaling were not indirectly caused by instability of FLS2 in these mutants.

To determine whether *PBL1* and *PBL2* also play a role in PAMP-induced responses, we identified homozygous T-DNA insertion mutants *pbl1* and *pbl2* (Figure S5F). Unlike *bik1*, which is smaller in size than WT (Veronese et al., 2006), the newly identified *pbl* mutants were morphologically normal (Figure S5G). As expected, the T-DNA insertion resulted in a near complete loss of *PBL1* and *PBL2* transcripts in *pbl1* and *pbl2* mutants, respectively (Figure S5H). These mutants were examined for PAMP-induced oxidative burst and callose deposition. *pbl1* and *pbl2* showed a small (~30%) but statistically significant reduction in flg22-induced H_2O_2 production compared with WT (Figure S5I). elf18-induced H_2O_2 production was reduced to ~40% in *pbl1* but was normal in the *pbl2* mutant (Figure S5J). The chitin-induced H_2O_2 production was largely normal in both *pbl1* and *pbl2* (Figure S5K). In addition, callose deposition in *pbl1* was normal upon flg22 treatment, but was significantly reduced when treated with elf18 and chitin (Figure S5L). *pbl2* showed significantly reduced callose deposition in flg22 and elf18 treatment, but was completely normal upon chitin treatment (Figure S5L). Taken together, these results indicate that *BIK1* and, to a lesser extent, *PBL1*, *PBL2*, and *PBS1*, are required for PTI defenses. We next constructed a *bik1/pbl1* double mutant. The flg22-induced oxidative burst and chitin-induced callose deposition were further reduced in the double mutant compared with the single mutants (Figures 5E and 5F), indicating that *BIK1* and *PBL1* act additively in PTI defenses.

BIK1 Is Required for PAMP-Induced Resistance to *P. syringae* Bacteria

A flg22-protection assay was carried out to determine whether *BIK1* is required for PAMP-induced resistance to *P. syringae* (Zipfel et al., 2004). Pretreatment of WT and *pbs1* plants with flg22 completely protected plants from subsequent infection by a virulent strain of *P. syringae* (Figure 6A). In contrast, flg22 pretreatment failed to enhance resistance to *P. syringae* in *bik1* plants. In the absence of flg22 treatment, the *bik1* mutant displayed elevated resistance to this strain (Veronese et al., 2006), likely because of heightened salicylic acid (SA) level in the *bik1* mutant, a phenotype that has also been reported for *bak1/bkk1* mutants (He et al., 2007). Nonetheless, flg22-treated *bik1* plants supported approximately 3- to 10-fold greater bacterial growth than did the flg22-treated WT plants. To further determine the role of *BIK1* in PAMP-induced resistance to *P. syringae*, we spray inoculated WT and *bik1* plants with a nonpathogenic mutant strain of *P. syringae*, *hrcC*$^-$, which carries a collection of PAMPs but lacks a functional type III secretion system. Strikingly, the *hrcC*$^-$ mutant bacteria grew 100-fold greater in *bik1* than in WT plants (Figure 6B). Similar experiments failed to detect altered bacterial growth in *pbs1*, *pbl1*, and *pbl2* mutants (data not shown). These results indicate that *BIK1* plays a major role in PAMP-induced resistance to *P. syringae*.

It may be argued that the high level of SA in the *bik1* mutant might have inhibited PTI defenses. However, this is highly unlikely because SA is known to positively regulate PTI defenses (Mishina and Zeier, 2007; Tsuda et al., 2008). We nonetheless

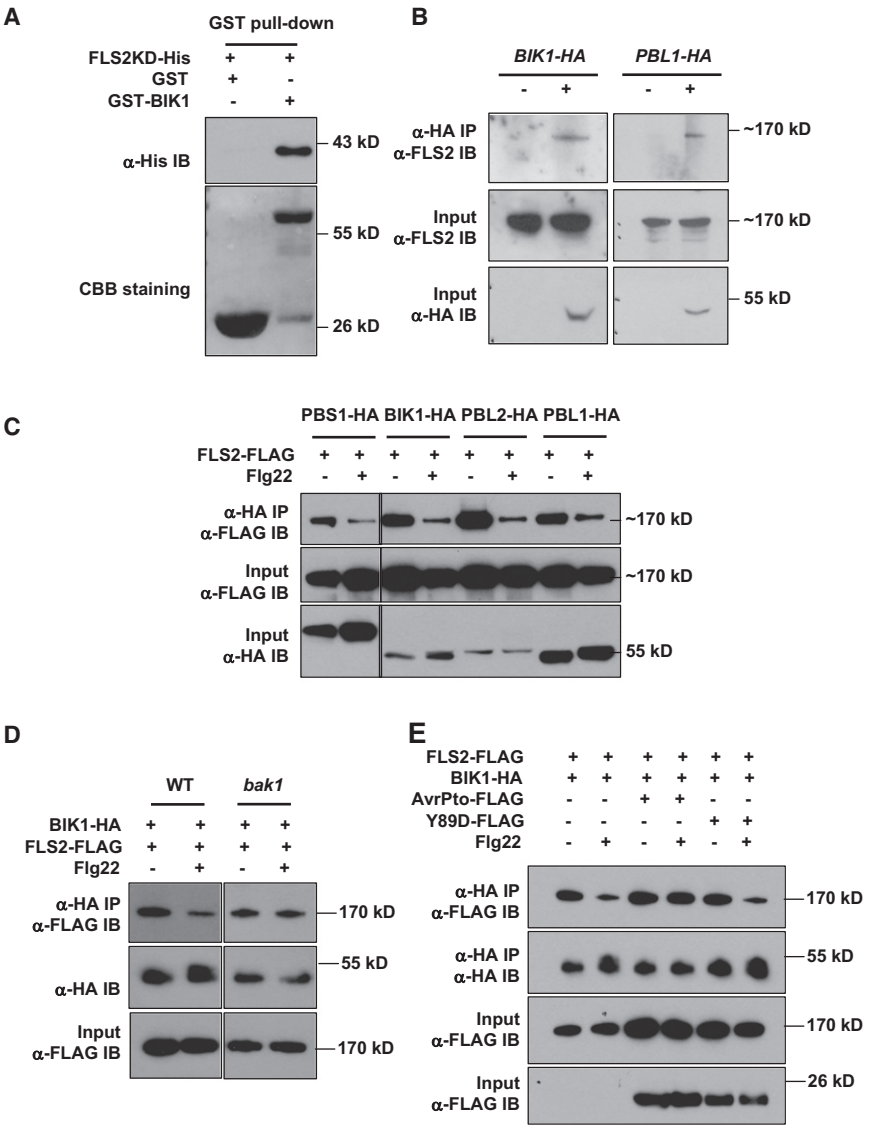

Figure 4. BIK1 and PBL1 Interact with Unstimulated FLS2

(A) BIK1 interacts with the kinase domain of FLS2 in vitro. GST pull-down assay was used to detect the interaction between GST-BIK1 and His-tagged FLS2 kinase domain (FLS2KD-His). The amount of FLS2KD-His was determined by anti-His immunoblot. Coomassie brilliant blue (CBB) staining indicates the amounts of GST or GST-BIK1 protein in the sample.

(B) BIK1 and PBL1 interact with FLS2 in plants. *rps5* plants with (+) or without (−) the *BIK1::BIK1-HA* or *PBL1::PBL1-HA* transgene were used for the co-IP (IP) assay. Total protein was immunoprecipitated with an anti-HA antibody, and the presence of BIK1-HA, PBL1-HA, and FLS2 in the immune complex was determined by immunoblot (IB) with the indicated antibodies.

(C–E) Protoplasts isolated from WT plants (C and E) or the indicated genotypes (D) were transfected with the indicated constructs and treated with flg22 before protein was isolated for the co-IP assay. The results shown are representative of three independent experiments.

(C) Flg22 induces dissociation of BIK1, PBS1, PBL1, and PBL2 from FLS2 in protoplasts.

(D) BAK1 is required for flg22-induced BIK1-FLS2 dissociation.

(E) AvrPto inhibits flg22-induced BIK1-FLS2 dissociation.

generated a *bik1/sid2* double mutant to determine whether the defects of PTI defenses in *bik1* were caused by elevated SA in this mutant. *SID2* encodes an isochorismate synthase that is critical for the pathogen-induced SA accumulation in plants (Wildermuth et al., 2001). Consistent with a positive role of SA in PTI defenses, the *sid2* mutant displayed reduced H_2O_2 production and callose deposition in response to flg22 (Figures S6A and S6B). The *bik1/sid2* double mutant was further compromised in these responses. Furthermore, bacterial growth assay showed that the *bik1/sid2* double mutant was not protected by flg22 treatment, compared with the normal protection in *sid2* and WT plants (Figure S6C). Taken together, these results demonstrated that *BIK1* is required for PAMP-induced resistance to *P. syringae* that is likely independent of SA accumulation.

BIK1 Phosphorylation Positively Regulates PAMP Signaling

To determine the role of BIK1 kinase activity in PAMP signaling, we introduced a lysine 105-to-glutamate substitution (K105E) into BIK1 and overexpressed this mutant in protoplasts. K105 is a conserved ATP-binding site and the mutation is expected to abolish kinase activity. Figure S7A shows that whereas the expression of the WT BIK1 constitutively induced *FRK1::LUC* reporter gene expression, the BIK1^{K105E} mutation (BIK1$^{K/E}$) blocked PAMP-induced *FRK1::LUC* expression (Figure 7A; Figure S7A), indicating that BIK1^{K105E} acted as a dominant-negative mutant in PTI signaling. Similarly, overexpression of the ATP-binding site mutant form of PBS1, PBL1, and PBL2 also inhibited PAMP-induced *FRK1::LUC* expression (Figure 7A). Interestingly, a BIK1$^{G230A/D231A}$ mutant (BIK1$^{GD/AA}$) in which the AvrPphB cleavage site was mutated also showed a dominant-negative effect when expressed in protoplasts, indicating that G230 and D231 are functionally important residues. Immunoblotting showed that these mutant proteins were expressed normally in protoplasts (Figure S7B). The FLAG-tagged WT *BIK1* and *BIK1^{K105E}* mutant were introduced into WT *Arabidopsis* plants as a stable transgene under the control of the estradiol-inducible promoter. T1 transgenic plants overaccumulating the WT and mutant BIK1 proteins (Figure S7C) were examined for flg22-induced oxidative burst. Whereas transgenic plants expressing the WT BIK1 (*BIK1OX*) were indistinguishable from nontransgenic controls, plants expressing BIK1^{K105E} (*K105EOX*) were greatly compromised in flg22-induced oxidative burst (Figure 7B). These results further support an additive role of the BIK1 family proteins in

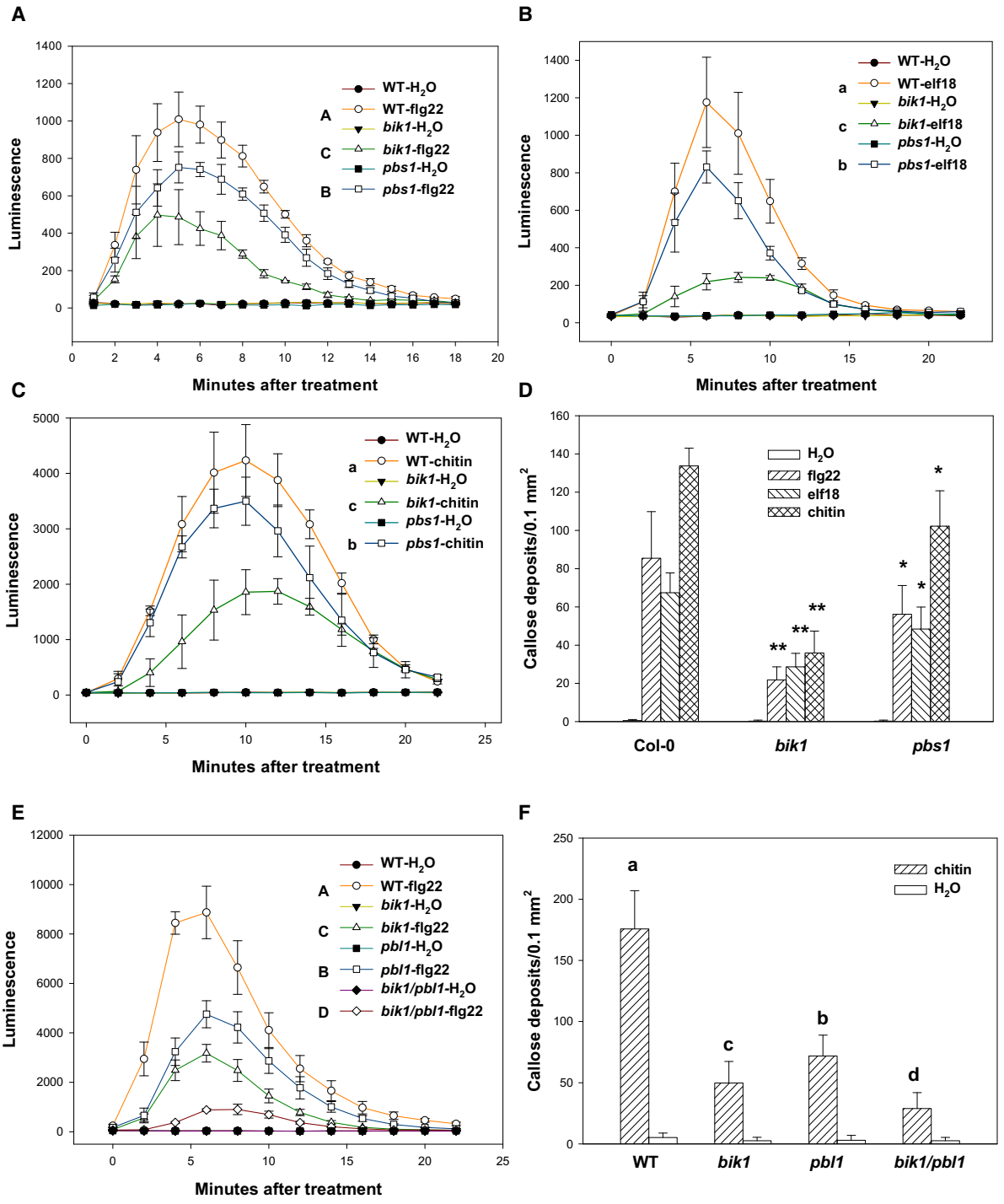

Figure 5. *BIK1* and *PBL1* Are Required for Defenses Triggered by Multiple PAMPs

(A–C) *bik1* and *pbs1* are compromised in PAMP-induced oxidative burst.

(D) *bik1* and *pbs1* are compromised in PAMP-induced callose deposition.

(E) Flg22-induced oxidative burst in WT, *bik1*, *pbl1*, and *bik1/pbl1* double mutant.

(F) Chitin-induced callose deposition in WT, *bik1*, *pbl1*, and *bik1/pbl1* double mutant. Error bars indicate standard deviation. Statistic analyses were carried out as in Figure 1. The results shown are representative of two to four independent experiments.

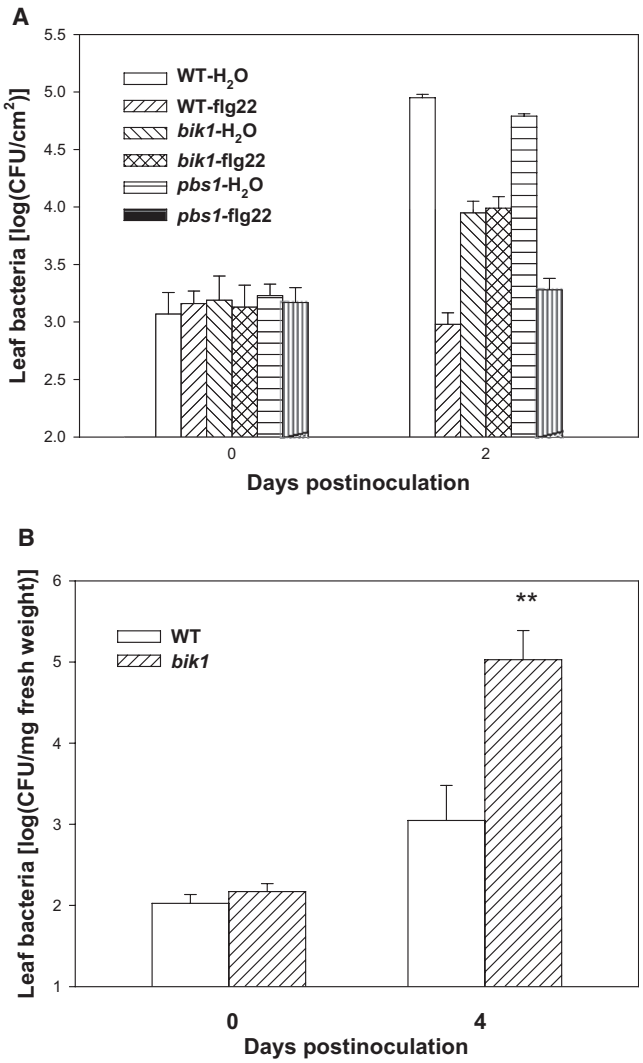

Figure 6. BIK1 Is Required for PAMP-Induced Resistance to *P. syringae*

(A) Flg22 fails to protect *bik1* plants from *P. syringae* infection. Plants of the indicated genotypes were pretreated with H_2O or flg22 for 1 day, infiltrated with *P. syringae* DC3000 bacteria, and the bacterial population in the leaf was determined at the indicated times.

(B) *bik1* supports greater multiplication of *P. syringae hrcC*$^-$ mutant bacteria. Plants of the indicated genotypes were spray inoculated with *P. syringae hrcC*$^-$ mutant bacteria, and the bacterial population in the leaf was determined at the indicated times. Error bars indicate standard deviation. Student's *t* test was carried out to determine the significance of the difference of *hrcC*$^-$ mutant bacterial growth between WT and *bik1* plants. ** indicates a significant difference at $p < 0.01$. The experiments were repeated four times with similar results.

PTI signaling and indicate that the kinase activity of these proteins is required for function.

Attempts to determine whether FLS2 directly phosphorylates BIK1 in vitro were unsuccessful, because recombinant FLS2 possessed only weak kinase activity. Nonetheless, the FLS2- and BAK1-dependent, flg22-induced phosphorylation of BIK1 prompted us to test the functional significance of BIK1 phosphorylation. Mass spectrometry analysis was carried out to determine phosphorylation sites in autophosphorylated BIK1. Because BIK1 is an RD kinase, which contains a conserved arginine immediately preceding the invariant aspartate in subdomain VI essential for catalytic activity, and the phosphorylation of the activation loop often is required for the activation of RD kinases (Nolen et al., 2004), we inspected potential phosphorylation sites in the activation loop. Indeed, a phosphorylated S236 in the activation loop was readily detected (Figure S7D). Site-directed mutagenesis was carried out to determine whether S236 is required for PAMP-induced *FRK1::LUC* expression. When expressed in protoplasts, BIK1^{S236A} acted as a dominant-negative mutant and strongly inhibited PAMP-induced *FRK1::LUC* expression (Figure 7C), indicating that S236 is important for signaling. We next determined whether S236 is required for flg22-induced phosphorylation of BIK1 in protoplasts. Whereas the majority of WT BIK1 becomes phosphorylated within 5 min of flg22 treatment, only a small proportion of BIK1^{S236A} is phosphorylated, indicating that S236 is required for optimum phosphorylation (Figure 7D). We reasoned that additional amino acids in the activation loop may be phosphorylated, and therefore constructed a quadruple mutant BIK1$^{SYST/AAAA}$ carrying S233A, Y234A, S236A, and T237A substitutions. Indeed, no phosphorylation was detected in the BIK1$^{SYST/AAAA}$ mutant (Figure S7E). Consistent with the possibility that additional residues in the activation loop are phosphorylated upon flg22 treatment, the BIK1^{T237A} mutant also acted as a dominant-negative mutant and inhibited PAMP-induced *FRK1::LUC* expression (Figure 7C).

BIK1-FLS2 Dissociation Is Not Required for FLS2-BAK1 Association

The dominant-negative effect of the BIK1^{K105E} mutant prompted us to determine whether the mutation affects BIK1-FLS2 interaction. Strikingly, the mutant showed stronger interaction with FLS2 in protoplasts (Figure S4D), and the flg22 treatment failed to induce its dissociation from FLS2. Our results in Figures 3 and 4 indicated that BAK1 is required for the flg22-induced phosphorylation of BIK1 and BIK1-FLS2 dissociation. We further explored the relationship between FLS2-BIK1 dissociation and FLS2-BAK1 association in protoplasts. The flg22 treatment induced a strong interaction between FLS2 and BAK1, as previously reported (Chinchilla et al., 2007; Heese et al., 2007), and coexpression of either WT BIK1 or the BIK1^{K105E} mutant did not inhibit FLS2-BAK1 association (Figure S4E), suggesting that a BIK1-FLS2 dissociation is not a prerequisite for FLS2-BAK1 association.

DISCUSSION

In this study, we show that the *P. syringae* effector AvrPphB can target multiple PBS1-like kinases and inhibit PTI defenses. Genetic analyses showed that BIK1 and, to a lesser extent, PBL1, PBL2, and PBS1, are required for signaling from multiple PAMPs. Protein-protein interaction and phosphorylation studies suggested that BIK1, and likely PBS1 and other PBL proteins, directly act downstream of FLS2, EFR, and CERK1 to trigger immune responses. Thus, the PBL and PBS1 proteins are key components that integrate signaling from multiple immune receptors.

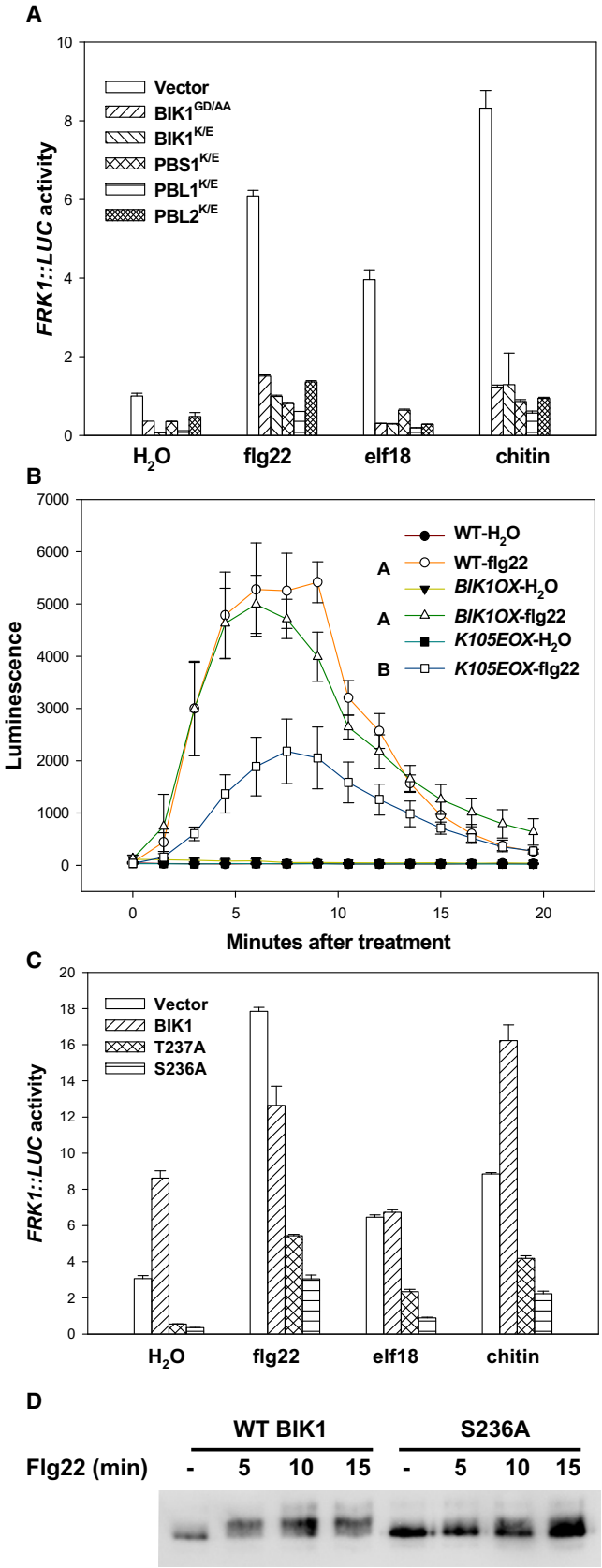

Figure 7. BIK1 Kinase Activity Positively Regulates PTI Signaling

(A) Transient expression of ATP-binding site mutant form of BIK1, PBS1, PBL1, and PBL2 inhibits PAMP-induced *FRK1::LUC* expression in protoplasts. WT protoplasts were transfected with *FRK1::LUC* along with the indicated constructs, induced with the indicated PAMPs for 3 hr, and *FRK1::LUC* activity was determined and normalized to internal *35S::RLUC* activity.

(B) Expression of ATP-binding site mutant form of *BIK1* inhibits flg22-induced oxidative burst in stable transgenic plants. Nontransgenic (WT) and T1 transgenic plants carrying the indicated transgene were induced with estradiol, and leaf strips were treated with flg22. H_2O_2 production was measured at the indicated times. Student's *t* test was carried out to determine the significance of the difference between flg22-treated WT, *BIK1OX*, and *K105EOX* transgenic plants. Different letters indicate significant difference at $p < 0.01$.

(C) Expression of BIK1 phosphorylation site mutants inhibits PAMP-induced *FRK1::LUC* expression in protoplasts. WT protoplasts were transfected with *FRK1::LUC* along with HA-tagged WT BIK1, $BIK1^{S236A}$, or $BIK1^{T237A}$, induced with the indicated PAMPs for 3 hr, and *FRK1::LUC* activity was determined. Error bars indicate standard deviation.

(D) S236 is required for optimum phosphorylation of BIK1. WT BIK1-HA and the $BIK1^{S236A}$-HA mutant were expressed in WT protoplasts and induced with flg22 for the indicated times. Protein was isolated by anti-HA immunoprecipitation and subjected to anti-HA immunoblot. The data shown are representative of two to three experiments.

In addition to PBS1, our analysis identified at least eight PBL proteins that are proteolytically cleaved by AvrPphB. A previous report suggested that recombinant AvrPphB specifically cleaves in vitro translated PBS1, but not its homologs (Shao et al., 2003). Either the recombinant AvrPphB protein is not fully active or the in vitro translated PBS1 homologs are not optimum for cleavage. BIK1 is localized to the plasma membrane (Veronese et al., 2006). PBS1 and many other PBL proteins may also localize to the plasma membrane, because these proteins possess putative myristoylation and palmitoylation sites at the N terminus (Figure S2A). Consistent with a role in targeting these kinases, AvrPphB is fatty acylated following autoproteolysis and localized to the plasma membrane (Dowen et al., 2009; Nimchuk et al., 2000). When directly expressed in plants, AvrPphB inhibited defenses triggered by flg22, elf18, and chitin. This is consistent with our findings that *bik1*, *pbl1*, *pbl2*, and *pbs1* mutants are compromised to varying degrees in defense responses induced by these PAMPs. Together, our results support that AvrPphB targets BIK1, and possibly PBS1 and other PBL proteins, to inhibit PTI.

It should be noted that AvrPphB is an effector from *P. syringae* pv *phaseolicola*, a nonadapted bacterium on *Arabidopsis*. Overexpression of AvrPphB in *Arabidopsis* protoplasts resulted in a significant but incomplete cleavage of BIK1. Delivery of AvrPphB from *P. syringae* bacteria only resulted in a cleavage of a small proportion of BIK1 in plants. These results explain the partial loss of PTI responses in stable *AvrPphB* transgenic plants and the inability to detect virulence activity on *Arabidopsis* plants when *avrPphB* is carried by the bacterium. One speculation is that a BIK1 ortholog in bean could be a better substrate for AvrPphB.

Our reverse genetic and molecular analyses demonstrate that BIK1 is an important component for integrating signaling from multiple PAMP receptors. The *bik1* mutant is greatly compromised in PAMP-induced oxidative burst and callose deposition. Most importantly, the *bik1* mutant is severely compromised in PAMP-induced resistance to *P. syringae* in flg22-protection

assays and *hrcC*$^{-}$ mutant bacteria spray-inoculation assays. *pbl1*, *pbl2*, and *pbs1* all exhibited small but statistically significant reduction in PTI defenses in response to one or more PAMPs, indicating that PBL1, PBL2, and PBS1 also contribute to PTI defense responses. Furthermore, a *bik1/pbl1* double mutant displayed greater defects in PTI defenses than did single mutants, indicating that *BIK1* and *PBL1* act additively in PAMP-induced defense responses.

The *bik1* mutant constitutively accumulates SA (Veronese et al., 2006). However, the increased SA level in *bik1* is not the cause of reduced PTI defenses in this mutant, for the reasons below. It was reported that PAMPs induce SA accumulation, and that SA is required for the expression of a portion of PAMP-response genes (Tsuda et al., 2008). This is consistent with our findings that the *sid2* mutant showed reduced callose deposition and oxidative burst in response to flg22 treatment (Figures S6A and S6B). In addition, the *ein3/eil1* double mutant constitutively accumulates SA and shows increased callose deposition in response to flg22 (Chen et al., 2009). These results clearly demonstrate a positive role of SA in PTI defenses. Indeed, introduction of the *sid2* mutation into *bik1* did not restore PTI defenses to *bik1*. Importantly, flg22-induced resistance to *P. syringae* bacteria was intact in the *sid2* mutant but abolished in the *bik1/sid2* double mutant (Figure S6C). Together, these results indicate that the reduction of PTI signaling in *bik1* was unlikely to be caused by the elevated SA in this mutant. The direct cause of SA accumulation in the *bik1* mutant is not known, but it is not uncommon that positive regulators of plant immunity also act to feedback inhibit SA biosynthesis. For instance, WRKY54 and WRKY70 positively regulate SA-response gene expression but also negatively regulate SA accumulation (Wang et al., 2006). Likewise, BAK1 is a positive regulator critically important for PTI signaling, but the *bak1/bkk1* double mutant exhibits SA-dependent cell death (He et al., 2007). It was recently shown that another receptor-like kinase, BIR1, interacts with BAK1 to negatively regulate cell death and SA accumulation (Gao et al., 2009). It may be that BIK1 also mediates BIR1-dependent SA regulation in addition to PAMP signaling.

BIK1 directly interacts with FLS2 in unstimulated plant cells and is phosphorylated upon stimulation by flg22 in an FLS2-dependent manner. Similarly, PBL1 also interacts with unstimulated FLS2 and is phosphorylated upon flg22 stimulation. AvrPto, which inhibits FLS2 kinase activity, blocks flg22-induced BIK1 phosphorylation and BIK1-FLS2 dissociation. The flg22-induced BAK1-FLS2 association is not affected by the ATP-binding site mutant form of BIK1, which does not dissociate from FLS2. In contrast, the flg22-induced phosphorylation of BIK1 and BIK1-FLS2 dissociation requires BAK1. Together, these results support the proposal that BIK1 acts downstream of FLS2 and BAK1. ATP-binding site and phosphorylation site mutant forms of BIK1 dominantly inhibit PTI defenses, indicating that the activated BIK1 kinase positively regulates PTI signaling. The flg22-induced phosphorylation of BIK1 and PBL1 and their dissociation from FLS2 are reminiscent of the ligand-induced BSK1 phosphorylation and dissociation from BRI1 in the brassinosteroid signaling pathway (Tang et al., 2008). It is possible that the dissociation of the phosphorylated BIK1 and PBL1 proteins from FLS2 allows the activation of other components downstream of BIK1 and PBL1.

Following the submission of this work, Lu et al. (2010) reported a flg22-induced phosphorylation of BIK1 which is largely consistent with our findings. By using co-IP assays in protoplasts, this work suggested that BIK1 can interact with FLS2 and BAK1. The BIK1-FLS2 interaction is consistent with our findings. Our co-IP assays showed a BIK1-BAK1 association only when FLS2 or EFR was overexpressed in the same protoplasts, suggesting that this association is indirect, at least in our analysis.

Our findings that AvrPphB targets the closely related kinases BIK1, PBL1, PBL2, and PBS1 provide insight into the evolution of RPS5-specified ETI. The *pbs1* mutant displayed marginal defects in PTI defenses. Unlike the *bik1* mutant, *pbs1* was not compromised in PAMP-induced resistance to *P. syringae*. The data are consistent with two models. In the first scenario, BIK1, PBL1, PBL2, and PBS1 are functionally additive, as suggested by the enhanced defects in PTI defenses in the *bik1/pbl1* double mutant. PBS1 may be an operational virulence target (van der Hoorn and Kamoun, 2008) that has evolved into a molecular sensor of AvrPphB (Dangl and Jones, 2001). The association of PBS1 with RPS5 allows the latter to trigger ETI upon sensing the cleavage-induced conformational change in PBS1 (Ade et al., 2007). Alternatively, PBS1 might have evolved from an ancestral protein that once was an important PTI signaling component, a possibility consistent with the normal PAMP-induced resistance to *P. syringae* in *pbs1*. The minor reduction of PTI defenses in *pbs1* may reflect residue activity of PBS1 in PTI signaling. In this scenario, PBS1 may act as a "decoy" by mimicking true virulence targets, such as BIK1, to trigger ETI (Zhou and Chai, 2008). Although further study is needed to test these models, our results strongly support the notion that ETI has evolved to detect the virulence activity of pathogen effectors.

EXPERIMENTAL PROCEDURES

Plant Materials

Arabidopsis thaliana plants used in this study include the WT (Col-0) and *rps5-2* (Warren et al., 1998), *bik1* (Veronese et al., 2006), *pbs1-2* (Warren et al., 1999), *cerk1* (Wan et al., 2008), *fls2* (Xiang et al., 2008), *efr* (Zipfel et al., 2006), and *pbl1* and *pbl2* (Figure S5F) mutants. *BIK1::BIK1-HA*, *PBL1::PBL1-HA*, and estradiol-inducible *AvrPphB-FLAG*, *BIK1-FLAG* (*BIK1OX*), and *BIK1*^{K105E}*-FLAG* (*K105EOX*) transgenic plants were generated as described in Supplemental Information.

Transient Expression and Reporter Assay in Protoplasts

Protoplasts isolated from 5-week-old plants were cotransfected with *FRK1::LUC* and *35S::RLUC* (Renilla luciferase) along with the indicated constructs. Twelve hours after transfection, protoplasts were treated with 1 μM flg22 or 1 μM elf18 or 200 μg/ml chitin. Protein was isolated 3 hr after PAMP treatment, and LUC activity was determined by using the Dual-Luciferase Reporter system (Promega) following the manufacturer's instructions.

Oxidative Burst

Five-week-old plant leaves were sliced into approximately 1 mm strips, incubated in H_2O in a 96-well plate for 12 hr, and treated with 1 μM flg22, 1 μM elf18, or 200 μg/ml chitin in 100 μl buffer containing 20 μM luminol and 1 μg/ml horseradish peroxidase (Sigma) as described (Zhang et al., 2007). Luminescence was recorded by using the GLOMAX 96 microplate luminometer (Promega). Each data point consists of at least four replicates. For experiments involving the *AvrPphB-FLAG* transgene, plants were pretreated with estradiol as described (Li et al., 2005) prior to the oxidative burst assay.

Callose Deposition

A seedling-based procedure for callose induction was adapted from Clay et al. (2009). Briefly, *Arabidopsis* seeds were germinated in a 12-well tissue-culture plate containing liquid MS medium at 23°C with 75% relative humidity under 16 hr daylight. Seedlings were transferred to fresh media on day 8, and 9-day-old seedlings were treated with H_2O, 1 μM flg22, 1 μM elf18, or 200 μg/ml chitin for 18 hr. Callose staining, image acquisition, and processing were carried out as described (Zhang et al., 2007). Each data point consists of five replicates.

Bacterial Growth Assay

For the flg22-protection assay, 5-week-old plants were first infiltrated with 1 μM flg22 or H_2O 1 day before infiltrating 10^6 cfu/ml *P. syringae* DC3000. Leaf bacterial number was determined at the indicated times after bacterial inoculation. Each data point consists of at least four replicates. For spray inoculation, plants were sprayed with an *hrcC*$^-$ mutant derived from DC3000 (Yuan and He, 1996) at 5×10^8 cfu/ml, and bacterial population in the leaf was determined at the indicated times.

GST Pull-Down Assay

GST or GST-BIK1 was expressed in *Escherichia coli*. Soluble protein was passed through a glutathione agarose column, washed five times with washing buffer (25 mM Tris-HCl [pH 7.5], 50 mM NaCl, 3 mM DTT). His-tagged FLS2 kinase domain (FLS2KD-His) was expressed in *E. coli* and purified by using an Ni-NTA column (Xiang et al., 2008). Equal amounts of purified FLS2KD-His were passed through a glutathione agarose column containing GST or GST-BIK1. The column was washed five times with washing buffer as above, and the bound protein was eluted with elution buffer (15 mM GSH, 25 mM Tris-HCl [pH 7.5], 50 mM NaCl, 3 mM DTT). The presence of FLS2KD-His was detected by an anti-His immunoblot.

Coimmunoprecipitation Assay

Total protein was extracted from 10-day-old *rps5*, *rps5/BIK1::BIK1-HA*, or *rps5/PBL1::PBL1-HA* transgenic plants (T2 generation) with extraction buffer (50 mM HEPES [pH 7.5], 150 mM KCl, 1 mM EDTA, 1 mM DTT, 0.2% Triton X-100, 1 mM PMSF). For anti-HA IP, total protein was precleared with protein A agarose (Upstate) for 1 hr, followed by precipitation with 2 μg anti-HA together with protein A agarose for 4 hr. For anti-FLAG IP, total protein was incubated with an agarose-conjugated anti-FLAG antibody for 4 hr. Immunoprecipitates were separated by 10% NuPAGE gel (Invitrogen), and the presence of FLS2, BIK1-HA, or PBL1-HA was detected by anti-FLS2 and anti-HA immunoblot. For co-IP experiments in protoplasts, the protoplasts were incubated for 12 hr after transfection, treated with either H_2O or 1 μM flg22 for 5–10 min, and total protein was extracted for co-IP. The presence of PBL-HA, PBS1-HA, BAK1-FLAG, FLS2-FLAG, EFR-FLAG, or CERK1-FLAG was detected by anti-HA and anti-FLAG immunoblot.

Detection of BIK1 and PBL1 Phosphorylation

WT or *fls2* protoplasts were transfected with BIK1-HA or PBL1-HA alone or together with FLS2-FLAG. The protoplasts were then treated with 1 μM flg22, and total protein was extracted at various time points with a buffer containing 50 mM HEPES (pH 7.5), 0.15 M NaCl, 1 mM EDTA, 5 mM sodium fluoride, 1 mM sodium vanadate, 1 mM DTT, 0.1% Triton X-100, and 1× proteinase inhibitor cocktail (Roche). Samples were separated by 10% NuPAGE gel (Invitrogen) and subjected to anti-HA immunoblot. For phosphatase treatment, total protein was treated with λ protein phosphatase (New England Biolabs) according to the manufacturer's instructions.

SUPPLEMENTAL INFORMATION

Supplemental Information includes Supplemental Experimental Procedures and seven figures and can be found with this article online at doi:10.1016/j.chom.2010.03.007.

ACKNOWLEDGMENTS

The authors thank Roger Innes and Jijie Chai for helpful comments. J.-M.Z. was supported by a grant from the Chinese Ministry of Science and Technology (2003-AA210080).

Received: December 9, 2009
Revised: January 20, 2010
Accepted: February 26, 2010
Published: April 21, 2010

REFERENCES

Abramovitch, R.B., Janjusevic, R., Stebbins, C.E., and Martin, G.B. (2006). Type III effector AvrPtoB requires intrinsic E3 ubiquitin ligase activity to suppress plant cell death and immunity. Proc. Natl. Acad. Sci. USA *103*, 2851–2856.

Ade, J., DeYoung, B.J., Golstein, C., and Innes, R.W. (2007). Indirect activation of a plant nucleotide binding site-leucine-rich repeat protein by a bacterial protease. Proc. Natl. Acad. Sci. USA *104*, 2531–2536.

Block, A., Li, G., Fu, Z.Q., and Alfano, J.R. (2008). Phytopathogen type III effector weaponry and their plant targets. Curr. Opin. Plant Biol. *11*, 396–403.

Chen, H., Xue, L., Chintamanani, S., Germain, H., Lin, H., Cui, H., Cai, R., Zuo, J., Tang, X., Li, X., et al. (2009). ETHYLENE INSENSITIVE3 and ETHYLENE INSENSITIVE3-LIKE1 repress SALICYLIC ACID INDUCTION DEFICIENT2 expression to negatively regulate plant innate immunity in *Arabidopsis*. Plant Cell *21*, 2527–2540.

Chinchilla, D., Bauer, Z., Regenass, M., Boller, T., and Felix, G. (2006). The *Arabidopsis* receptor kinase FLS2 binds flg22 and determines the specificity of flagellin perception. Plant Cell *18*, 465–476.

Chinchilla, D., Zipfel, C., Robatzek, S., Kemmerling, B., Nürnberger, T., Jones, J.D., Felix, G., and Boller, T. (2007). A flagellin-induced complex of the receptor FLS2 and BAK1 initiates plant defence. Nature *448*, 497–500.

Clay, N.K., Adio, A.M., Denoux, C., Jander, G., and Ausubel, F.M. (2009). Glucosinolate metabolites required for an *Arabidopsis* innate immune response. Science *323*, 95–101.

Cunnac, S., Lindeberg, M., and Collmer, A. (2009). *Pseudomonas syringae* type III secretion system effectors: repertoires in search of functions. Curr. Opin. Microbiol. *12*, 53–60.

Dangl, J.L., and Jones, J.D. (2001). Plant pathogens and integrated defence responses to infection. Nature *411*, 826–833.

Dowen, R.H., Engel, J.L., Shao, F., Ecker, J.R., and Dixon, J.E. (2009). A family of bacterial cysteine protease type III effectors utilize acylation-dependent and -independent strategies to localize to plasma membranes. J. Biol. Chem. *284*, 15867–15879.

Felix, G., Duran, J.D., Volko, S., and Boller, T. (1999). Plants have a sensitive perception system for the most conserved domain of bacterial flagellin. Plant J. *18*, 265–276.

Fu, Z.Q., Guo, M., Jeong, B.R., Tian, F., Elthon, T.E., Cerny, R.L., Staiger, D., and Alfano, J.R. (2007). A type III effector ADP-ribosylates RNA-binding proteins and quells plant immunity. Nature *447*, 284–288.

Gao, M., Wang, X., Wang, D., Xu, F., Ding, X., Zhang, Z., Bi, D., Cheng, Y.T., Chen, S., Li, X., and Zhang, Y. (2009). Regulation of cell death and innate immunity by two receptor-like kinases in *Arabidopsis*. Cell Host Microbe *6*, 34–44.

Gimenez-Ibanez, S., Hann, D.R., Ntoukakis, V., Petutschnig, E., Lipka, V., and Rathjen, J.P. (2009). AvrPtoB targets the LysM receptor kinase CERK1 to promote bacterial virulence on plants. Curr. Biol. *19*, 423–429.

Göhre, V., Spallek, T., Häweker, H., Mersmann, S., Mentzel, T., Boller, T., de Torres, M., Mansfield, J.W., and Robatzek, S. (2008). Plant pattern-recognition receptor FLS2 is directed for degradation by the bacterial ubiquitin ligase AvrPtoB. Curr. Biol. *18*, 1824–1832.

Gómez-Gómez, L., Felix, G., and Boller, T. (1999). A single locus determines sensitivity to bacterial flagellin in *Arabidopsis thaliana*. Plant J. *18*, 277–284.

He, K., Gou, X., Yuan, T., Lin, H., Asami, T., Yoshida, S., Russell, S.D., and Li, J. (2007). BAK1 and BKK1 regulate brassinosteroid-dependent growth and brassinosteroid-independent cell-death pathways. Curr. Biol. *17*, 1109–1115.

Heese, A., Hann, D.R., Gimenez-Ibanez, S., Jones, A.M., He, K., Li, J., Schroeder, J.I., Peck, S.C., and Rathjen, J.P. (2007). The receptor-like kinase SERK3/BAK1 is a central regulator of innate immunity in plants. Proc. Natl. Acad. Sci. USA *104*, 12217–12222.

Ichimura, K., Casais, C., Peck, S.C., Shinozaki, K., and Shirasu, K. (2006). MEKK1 is required for MPK4 activation and regulates tissue-specific and temperature-dependent cell death in *Arabidopsis*. J. Biol. Chem. *281*, 36969–36976.

Janjusevic, R., Abramovitch, R.B., Martin, G.B., and Stebbins, C.E. (2006). A bacterial inhibitor of host programmed cell death defenses is an E3 ubiquitin ligase. Science *311*, 222–226.

Jones, J.D., and Dangl, J.L. (2006). The plant immune system. Nature *444*, 323–329.

Kim, M.G., da Cunha, L., McFall, A.J., Belkhadir, Y., DebRoy, S., Dangl, J.L., and Mackey, D. (2005). Two *Pseudomonas syringae* type III effectors inhibit RIN4-regulated basal defense in *Arabidopsis*. Cell *121*, 749–759.

Kunze, G., Zipfel, C., Robatzek, S., Niehaus, K., Boller, T., and Felix, G. (2004). The N terminus of bacterial elongation factor Tu elicits innate immunity in *Arabidopsis* plants. Plant Cell *16*, 3496–3507.

Li, X., Lin, H., Zhang, W., Zou, Y., Zhang, J., Tang, X., and Zhou, J.-M. (2005). Flagellin induces innate immunity in nonhost interactions that is suppressed by *Pseudomonas syringae* effectors. Proc. Natl. Acad. Sci. USA *102*, 12990–12995.

Lu, D., Wu, S., Gao, X., Zhang, Y., Shan, L., and He, P. (2010). A receptor-like cytoplasmic kinase, BIK1, associates with a flagellin receptor complex to initiate plant innate immunity. Proc. Natl. Acad. Sci. USA *107*, 496–501.

Mishina, T.E., and Zeier, J. (2007). Pathogen-associated molecular pattern recognition rather than development of tissue necrosis contributes to bacterial induction of systemic acquired resistance in *Arabidopsis*. Plant J. *50*, 500–513.

Miya, A., Albert, P., Shinya, T., Desaki, Y., Ichimura, K., Shirasu, K., Narusaka, Y., Kawakami, N., Kaku, H., and Shibuya, N. (2007). CERK1, a LysM receptor kinase, is essential for chitin elicitor signaling in *Arabidopsis*. Proc. Natl. Acad. Sci. USA *104*, 19613–19618.

Mucyn, T.S., Clemente, A., Andriotis, V.M., Balmuth, A.L., Oldroyd, G.E., Staskawicz, B.J., and Rathjen, J.P. (2006). The tomato NBARC-LRR protein Prf interacts with Pto kinase in vivo to regulate specific plant immunity. Plant Cell *18*, 2792–2806.

Nimchuk, Z., Marois, E., Kjemtrup, S., Leister, R.T., Katagiri, F., and Dangl, J.L. (2000). Eukaryotic fatty acylation drives plasma membrane targeting and enhances function of several type III effector proteins from *Pseudomonas syringae*. Cell *101*, 353–363.

Nolen, B., Taylor, S., and Ghosh, G. (2004). Regulation of kinases: controlling activity through activation segment conformation. Mol. Cell *15*, 661–675.

Nomura, K., DebRoy, S., Lee, Y.H., Pumplin, N., Jones, J., and He, S.Y. (2006). A bacterial virulence protein suppresses host immunity to cause plant disease. Science *313*, 220–223.

Qiu, J.L., Fiil, B.K., Petersen, K., Nielsen, H.B., Botanga, C.J., Thorgrimsen, S., Palma, K., Suarez-Rodriguez, M.C., Sandbech-Clausen, S., Lichota, J., et al. (2008). *Arabidopsis* MAP kinase 4 regulates gene expression through transcription factor release in the nucleus. EMBO J. *27*, 2214–2221.

Schwessinger, B., and Zipfel, C. (2008). News from the frontline: recent insights into PAMP-triggered immunity in plants. Curr. Opin. Plant Biol. *11*, 389–395.

Shan, L., He, P., Li, J., Heese, A., Peck, S.C., Nürnberger, T., Martin, G.B., and Sheen, J. (2008). Bacterial effectors target the common signaling partner BAK1 to disrupt multiple MAMP receptor-signaling complexes and impede plant immunity. Cell Host Microbe *4*, 17–27.

Shao, F., Golstein, C., Ade, J., Stoutemyer, M., Dixon, J.E., and Innes, R.W. (2003). Cleavage of *Arabidopsis* PBS1 by a bacterial type III effector. Science *301*, 1230–1233.

Suarez-Rodriguez, M.C., Adams-Phillips, L., Liu, Y., Wang, H., Su, S.H., Jester, P.J., Zhang, S., Bent, A.F., and Krysan, P.J. (2007). MEKK1 is required for flg22-induced MPK4 activation in *Arabidopsis* plants. Plant Physiol. *143*, 661–669.

Tang, X., Frederick, R.D., Zhou, J.-M., Halterman, D.A., Jia, Y., and Martin, G.B. (1996). Initiation of plant disease resistance by physical interaction of AvrPto and Pto kinase. Science *274*, 2060–2063.

Tang, W., Kim, T.W., Oses-Prieto, J.A., Sun, Y., Deng, Z., Zhu, S., Wang, R., Burlingame, A.L., and Wang, Z.Y. (2008). BSKs mediate signal transduction from the receptor kinase BRI1 in *Arabidopsis*. Science *321*, 557–560.

Tsuda, K., Sato, M., Glazebrook, J., Cohen, J.D., and Katagiri, F. (2008). Interplay between MAMP-triggered and SA-mediated defense responses. Plant J. *53*, 763–775.

van der Hoorn, R.A.L., and Kamoun, S. (2008). From guard to decoy: a new model for perception of plant pathogen effectors. Plant Cell *20*, 2009–2017.

Veronese, P., Nakagami, H., Bluhm, B., Abuqamar, S., Chen, X., Salmeron, J., Dietrich, R.A., Hirt, H., and Mengiste, T. (2006). The membrane-anchored BOTRYTIS-INDUCED KINASE1 plays distinct roles in *Arabidopsis* resistance to necrotrophic and biotrophic pathogens. Plant Cell *18*, 257–273.

Wan, J., Zhang, X., Neece, D., Ramonell, K.M., Clough, S., Kim, S., Stacey, M.G., and Stacey, G. (2008). A LysM receptor-like kinase plays a critical role in chitin signaling and fungal resistance in *Arabidopsis*. Plant Cell *20*, 471–481.

Wang, D., Amornsiripanitch, N., and Dong, X. (2006). A genomic approach to identify regulatory nodes in the transcriptional network of systemic acquired resistance in plants. PLoS Pathog. *2*, e123.

Warren, R.F., Henk, A., Mowery, P., Holub, E., and Innes, R.W. (1998). A mutation within the leucine-rich repeat domain of the *Arabidopsis* disease resistance gene *RPS5* partially suppresses multiple bacterial and downy mildew resistance genes. Plant Cell *10*, 1439–1452.

Warren, R.F., Merritt, P.M., Holub, E., and Innes, R.W. (1999). Identification of three putative signal transduction genes involved in *R* gene-specified disease resistance in *Arabidopsis*. Genetics *152*, 401–412.

Wildermuth, M.C., Dewdney, J., Wu, G., and Ausubel, F.M. (2001). Isochorismate synthase is required to synthesize salicylic acid for plant defence. Nature *414*, 562–565.

Xiang, T., Zong, N., Zou, Y., Wu, Y., Zhang, J., Xing, W., Li, Y., Tang, X., Zhu, L., Chai, J., and Zhou, J.-M. (2008). *Pseudomonas syringae* effector AvrPto blocks innate immunity by targeting receptor kinases. Curr. Biol. *18*, 74–80.

Yuan, J., and He, S.Y. (1996). The *Pseudomonas syringae* Hrp regulation and secretion system controls the production and secretion of multiple extracellular proteins. J. Bacteriol. *178*, 6399–6402.

Zhang, J., Shao, F., Li, Y., Cui, H., Chen, L., Li, H., Zou, Y., Lan, L., Chai, J., Tang, X., and Zhou, J.-M. (2007). A *Pseudomonas syringae* effector inactivates MAPKs to suppress PAMP-induced immunity in plants. Cell Host Microbe *1*, 175–185.

Zhou, J.-M., and Chai, J.J. (2008). Plant pathogenic bacterial type III effectors subdue host responses. Curr. Opin. Microbiol. *11*, 179–185.

Zipfel, C., Robatzek, S., Navarro, L., Oakeley, E.J., Jones, J.D., Felix, G., and Boller, T. (2004). Bacterial disease resistance in *Arabidopsis* through flagellin perception. Nature *428*, 764–767.

Zipfel, C., Kunze, G., Chinchilla, D., Caniard, A., Jones, J.D., Boller, T., and Felix, G. (2006). Perception of the bacterial PAMP EF-Tu by the receptor EFR restricts *Agrobacterium*-mediated transformation. Cell *125*, 749–760.